

Coherent Elastic Neutrino-Nucleus Scattering (CEvNS) with COHERENT at the Spallation Neutron Source: A White Paper for the NSAC Long-Range Plan

COHERENT collaboration

November 26, 2022

Abstract

This white paper briefly describes the opportunities for measurement of coherent elastic neutrino-nucleus scattering (CEvNS) with the COHERENT experiment at Oak Ridge National Laboratory's Spallation Neutron Source. It is a companion to a separate white paper describing opportunities for inelastic neutrino-nucleus scattering measurements with COHERENT.

1 Summary Points for the NSAC LRP

- Measurement of CEvNS provides unique opportunities, including precision tests of the standard model (SM). Measurements on multiple nuclear targets are desirable for SM tests.
- In the few-percent uncertainty regime, measurements of neutron form factors of the nuclear target are feasible. For these, neutrino energies in the tens of MeV range are especially desirable.
- Stopped-pion neutrinos, with a well-understood flavor composition, time structure, and spectrum with energies up to ~ 50 MeV, provide a sweet spot for CEvNS measurements. Pulsed sources provide an excellent steady-state background reduction.
- The Oak Ridge National Laboratory (ORNL) Spallation Neutron Source (SNS) is the world's best source of stopped-pion neutrinos.
- The COHERENT program has been very successful in Neutrino Alley at the ORNL SNS First Target Station (FTS), with the first-light CEvNS measurement on CsI and a second measurement on argon (Ar). These are the only measurements of CEvNS so far. More CEvNS measurements on additional targets are ongoing, and more are planned for the next decade in Neutrino Alley.
- The SNS Second Target Station will offer even broader opportunities.
- Nuclear recoil quenching factors impact the observed CEvNS recoil spectrum and rate. There is a dedicated beam-line at the Triangle Universities Nuclear Laboratory for measuring quenching factors important for COHERENT, as well as the broader CEvNS community.
- COHERENT's program should be a key part of the Fundamental Symmetries, Neutrons, and Neutrinos Long Range Plan.

2 Coherent Elastic Neutrino-Nucleus Scattering

Coherent elastic neutrino-nucleus scattering (CEvNS) is a neutral-current weak interaction in which a neutrino interacts with a nucleus with low momentum transfer, such that the nucleon wavefunctions are in phase with each other and the nuclear recoils as an intact entity. The sole experimental signature of CEvNS is the tiny energy deposition of the recoiling nucleus, with maximum recoil energy $T \sim \frac{2E_\nu^2}{M}$, where E_ν is the neutrino energy and M the mass of the nucleus. The existence of the interaction was first predicted in 1974 [1].

The COHERENT experiment in Neutrino Alley exploited the SNS neutrino source [2] to make the first-light measurement of CEvNS on CsI [3] in 2017, and followed this with the first measurement of

CEvNS on argon in 2020 [4], as well as a measurement with a doubled CsI dataset [5] and improved understanding of detector response [6]. The current status is shown in Fig. 1.

The differential cross section of CEvNS predicted by the Standard Model is given by [7]

$$\frac{d\sigma}{dT}(T, E_\nu) = \frac{G_F^2 M}{2\pi} \left[(G_V + G_A)^2 + (G_V - G_A)^2 \left(1 - \frac{T}{E_\nu}\right)^2 - (G_V^2 - G_A^2) \frac{MT}{E_\nu^2} \right], \quad (1)$$

where T is the recoil energy, E_ν is the incident neutrino energy, G_F is the Fermi constant, M is the target nuclear mass,

$$G_V = (g_V^p Z + g_V^n N) F_{nucl}^V(Q^2), \quad (2)$$

$$G_A = (g_A^p (Z_+ - Z_-) + g_A^n (N_+ - N_-)) F_{nucl}^A(Q^2), \quad (3)$$

The parameters $g_V^{n,p}$ and $g_A^{n,p}$ are vector and axial-vector coupling factors, respectively, for protons and neutrons, Z and N are the proton and neutron numbers, Z_\pm and N_\pm refer to the number of spin up or down nucleons, $F_{nucl}^{V,A}$ are vector and axial nuclear form factors, and Q is the momentum transfer. As the numbers of spin up and down nucleons in a nucleus are either precisely zero or much smaller than the number of nucleons, the axial-vector contribution G_A is small. The couplings are subject to percent-level Q -dependent radiative corrections [8], with values of $g_V^n \sim -0.511$ and $g_V^p \sim 0.03$. The vector contribution G_V is hence mainly determined by the total number of neutrons in the target nucleus, so that the cross section scales approximately as the square of N , as shown in Fig. 1.

The observed energy deposited by nuclear recoils in scintillation- and ionization-based detectors is quenched. This quenching is energy-dependent, and must be measured to accurately predict the CEvNS recoil spectrum and observed CEvNS rate above detector threshold. Using the Triangle Universities Nuclear Laboratory Tandem Van de Graaff accelerator, quenching factors have been measured for several of COHERENT’s detectors [6, 9, 10, 11]. High-precision measurements of quenching factors for COHERENT’s targets will become important as neutrino flux uncertainties improve.

3 CEvNS Physics Opportunities

The measurement of CEvNS offers numerous physics opportunities, as a test of the standard model, as a probe of nuclear structure, as a tool for astrophysical measurements, and more. We describe briefly some highlights of a CEvNS physics program here, with emphasis on the reach of the COHERENT program. More information can be found in Refs. [12, 13] and references therein.

3.1 CEvNS as a Precision Standard Model Test

In the context of the standard model, CEvNS rates can be used to infer the weak mixing angle. The nuclear uncertainties for CEvNS calculations are relatively small. They enter into the event rate and spectrum via the form factor $F(Q)$ of equation 1, that describes the non-pointlike distribution of nucleons in the nucleus. The form factor is in general different for protons and neutrons, and also for axial and vector contributions to the interaction; however for CEvNS, the neutrons and vector contributions dominate and the standard approximation is to assume that the form factors are identical. Uncertainties on the CEvNS rate due to uncertainties on the form factor are at the few percent level. Therefore, a measurement of the CEvNS rate and energy distribution is a standard model test to the percent level. A variety of beyond-the-standard-model physics would enhance or suppress the total rate (for new heavy mediators) or distort the recoil spectrum (new light mediators). An anomalous neutrino magnetic moment would create an enhancement in cross section at low T . Sterile neutrino oscillations would result in a baseline- and recoil-energy-dependent distortion of the spectrum. These new physics scenarios may affect the separate neutrino flavors differently, highlighting the importance of multiple flavors in the SNS flux. Ref. [12] reviews some possibilities.

As well as potentially harboring signals of beyond-the-SM physics, CEvNS also can be a background for new physics searches, and hence must be understood. For example, relic dark matter searches will be blinded in the long term by CEvNS signals from natural neutrino sources (the so-called “neutrino floor” or “fog” [15]). Dark matter signals at accelerators are also limited by CEvNS backgrounds.

3.2 Nuclear Physics with CEvNS

Nuclear uncertainties at the few percent level enable new physics searches if overall CEvNS uncertainties are a larger level, as is currently the case. As uncertainties diminish, it will be possible to put useful

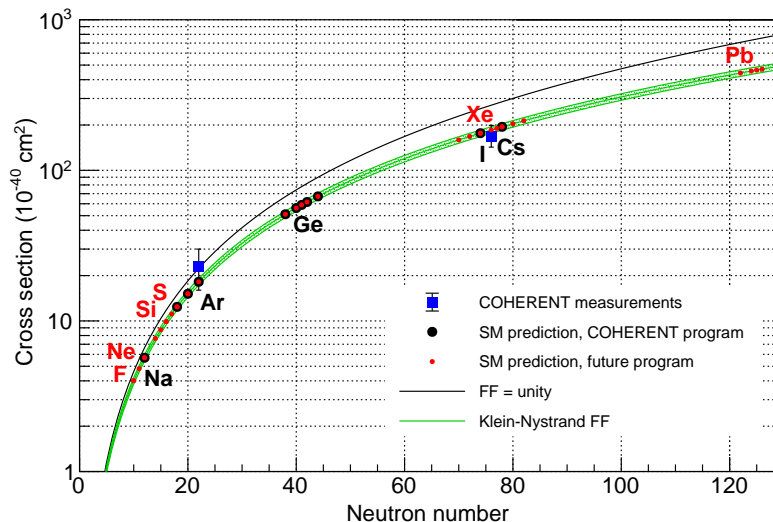


Figure 1: Flux-averaged CEvNS cross sections as a function of neutron number, from Ref. [14], with several potential future nuclear targets highlighted in red. These are not intended to be a comprehensive set, but rather several examples for which particular, known-to-be-feasible detector technologies have been proposed for CEvNS measurements.

constraints on nuclear form-factor parameters. A non-unity nuclear form factor results in a Q -dependent suppression of the CEvNS recoil rate. Because the weak charge is dominated by neutrons, it’s the neutron form factor that’s accessible with CEvNS— one can measure the neutron radius [16], and hence, in combination with proton radius data, one can infer the “neutron skin” width of the target nucleus.

The current uncertainties from CEvNS are not competitive with other methods for measuring neutron radii, such as PVES (electroweak parity-violating electron scattering). In the longer term, percent level precision on neutron radii will be achievable with CEvNS.

3.3 CEvNS for Astrophysics

In an end-of-life supernova, a massive star’s iron core will collapse to a compact remnant such as a neutron star or black hole. In most cases, this collapse produces a violent explosion in electromagnetic radiation and kinetic energy and, likely in all cases, a brilliant $\sim 10^{53}$ erg burst of neutrinos over a few tens of seconds. These supernova-burst neutrinos come in all flavors. Most are emitted quasi-thermally with energies of a few tens of MeV [17]. The flavor, energy, and time structure of the neutrino burst, measured by terrestrial detectors [18, 17], carries information about the astrophysics of the collapse, the remnant, and the subsequent explosion. It also carries information about the properties of neutrinos themselves, including information about neutrino mass ordering and flavor transitions within the star. Neutrinos ejected during core collapse are governed by complex and still somewhat uncertain stellar processes [19, 20]. Early in the explosion, the core density of the proto-neutron star is so high that neutrinos become trapped and thermalize, largely through coherent scattering [21]. Thus, the rate of neutrino diffusion from the core depends on the CEvNS rate. Furthermore, terrestrial neutrino and dark matter detectors can measure the muon and tau flavor components’ burst flux, for which energies are below the charged-current threshold and hence are solely accessible via neutral-current (NC) interactions like CEvNS. Beyond-the-standard model interactions, if present, could have a non-negligible effect on both modeling and detection.

Another astrophysical application is connected to neutron form-factor measurements possible with CEvNS, which enable constraint of the neutron star equation of state [22, 23] and other properties of astrophysical compact objects [24, 25].

4 Neutrinos at the Spallation Neutron Source

A variety of neutrino sources have been proposed for CEvNS studies. Reactors can produce very large neutrino fluxes, but with very low recoil energies. Pion decay-at-rest sources, such as the SNS, offer higher-energy neutrinos (up to about 53 MeV, dictated by the decay kinematics) with a pulsed time structure that facilitates background reduction.

Briefly, at a source like the present-day SNS, the impact of a pulse of accelerated protons on a mercury target produces (on average) about 0.0875 π^+ per proton. Each π^+ stops in the dense target, and decays via $\pi^+ \rightarrow \mu^+ + \nu_\mu$. The μ^+ comes to a rest in turn, and decays via $\mu^+ \rightarrow e^+ + \nu_e + \bar{\nu}_\mu$. The ν_e and $\bar{\nu}_\mu$ neutrinos are delayed relative to the prompt ν_μ by the characteristic 2.2- μ s muon lifetime [2].

Current SNS operations focus on a single target, liquid mercury at the FTS, which receives a pulsed, 1.4 MW proton beam of about 1 GeV at 60 Hz. A proton power upgrade, currently underway, will double the beam power by 2028, increasing the beam energy to 1.3 GeV and the average beam current to 38 mA.

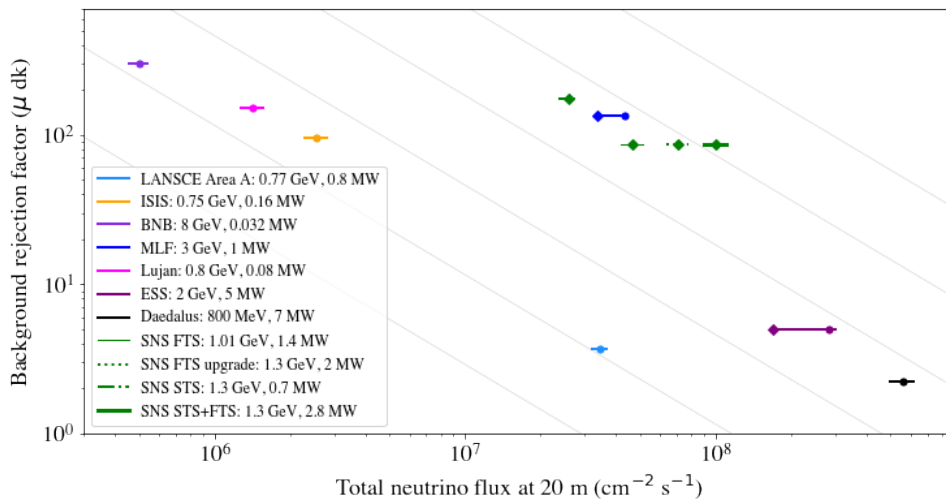


Figure 2: Figures of merit for stopped-pion neutrino sources worldwide (past, current and future). The x-axis shows the total (all-flavor) neutrino flux depending on the beam power, proton energy and details of the target geometry. The uncertainty is shown as the range of fluxes. The diamonds show flux estimates based on Geant4 QGSP_BERT; the circles indicate the relevant collaboration’s chosen baseline flux estimate. The y-axis shows the inverse square root of the duty factor, a measure of impact of background rejection due to beam pulsing, where duty factor is determined from the maximum of the muon decay lifetime, 2.2 μ s, and the beam pulse window. A larger value corresponds to improved steady-state background rejection. The diagonal lines represent contours of equal flux over inverse square root of the duty factor, an approximate overall figure of merit.

5 The COHERENT Program

COHERENT’s program is briefly summarized here. Detectors with sensitivity to inelastic neutrino interactions are described in Ref. [26].

5.1 COHERENT in Neutrino Alley at the SNS First Target Station

COHERENT presently operates in Neutrino Alley, a basement corridor at the FTS which provides substantial shielding against neutrons. The multiple detector deployments— past, present and future— are summarized in Tab. 1. The first-light result was on CsI in 2017, with full dataset results reported in 2021; a second measurement on Ar followed in 2020. COHERENT is currently deploying Ge and NaI

detectors as well as a tonne-scale Ar follow-on. A cryogenic CsI detector is also proposed. Various other target nuclei are under consideration for a future program— see Fig. 1.

Table 1: Parameters of COHERENT subsystems for CEvNS detection (past, current and near-term future). From Ref. [13].

Nuclear target	Detector Technology	Target Mass (kg)	Distance from source	Energy threshold (keV [†])	Deployment dates
CsI[Na]	Scintillating crystal	14	20 m	5	2015-2019
Ar	Single-phase LAr★	24	29 m	20	2016-2021
Ge	HPGe PPC [‡]	18	22 m	<5	2022
NaI[Tl]	Scintillating Crystal	3500	22 m	13	2022
Ar	Single-phase LAr★	750	29 m	20	2025
Ge	HPGe PPC [‡]	50	22 m	<5	2025
CsI	CsI+SiPM arrays at 40 K	10~15	20 m	1.4	2025

Finished Planned, ★liquid argon, ‡*p*-type point-contact, † nuclear recoil energy, approximate threshold

5.2 Opportunities at the SNS Second Target Station

In the coming years, the SNS will begin construction on a second target station (STS), with its own experimental hall. The STS target, a rotating array of tungsten wedges, will eventually receive every fourth proton pulse. Once nominal operations are underway, the FTS will thus undergo a 45 Hz proton beam while the STS receives a 15 Hz beam. See Fig. 3.

Space available in Neutrino Alley, while of high quality in terms of background reduction, is limited. More capacious facilities can be available at the STS in the early 2030’s, allowing for the deployment of larger detectors for precision CEvNS studies [27].

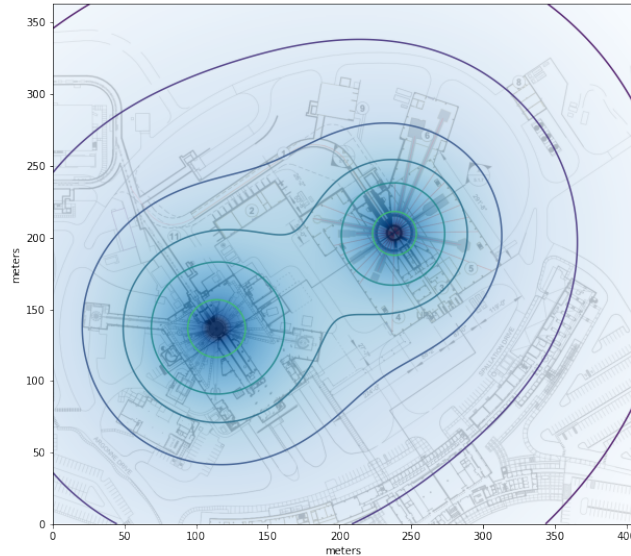


Figure 3: Left: Total neutrino flux emitted from the FTS and STS at 2.4 MW, as a function of position, showing also iso-flux contours.

6 Resources Required and Ask from the LRP Process

Costs for COHERENT detector deployments have been of the order of a few \$M each. The COHERENT program has so far been funded by a variety of sources, including substantial funding from the Department of Energy Office of High Energy Physics and the National Science Foundation in the U.S.. The physics of COHERENT falls at the boundary of high energy physics and nuclear physics, and several topics can be assigned quite squarely to the nuclear physics domain. We appeal for the LRP Process to recognize that COHERENT's physics occupies a region of overlap between areas traditionally stewarded by DOE OHEP and ONP, and ask for support for COHERENT's nuclear-physics-relevant program.

References

- [1] Daniel Z. Freedman. Coherent Neutrino Nucleus Scattering as a Probe of the Weak Neutral Current. *Phys. Rev. D*, 9:1389–1392, 1974.
- [2] D. Akimov et al. Simulating the neutrino flux from the Spallation Neutron Source for the COHERENT experiment. *Phys. Rev. D*, 106(3):032003, 2022.
- [3] D. Akimov et al. Observation of Coherent Elastic Neutrino-Nucleus Scattering. *Science*, 357(6356):1123–1126, 2017.
- [4] D. Akimov et al. First Measurement of Coherent Elastic Neutrino-Nucleus Scattering on Argon. *Phys. Rev. Lett.*, 126(1):012002, 2021.
- [5] D. Akimov et al. Measurement of the Coherent Elastic Neutrino-Nucleus Scattering Cross Section on CsI by COHERENT. *Phys. Rev. Lett.*, 129(8):081801, 2022.
- [6] D. Akimov et al. Measurement of scintillation response of CsI[Na] to low-energy nuclear recoils by COHERENT. *JINST*, 17(10):P10034, 2022.
- [7] J. Barranco, O. G. Miranda, and T. I. Rashba. Probing new physics with coherent neutrino scattering off nuclei. *JHEP*, 12:021, 2005.
- [8] Oleksandr Tomalak, Pedro Machado, Vishvas Pandey, and Ryan Plestid. Flavor-dependent radiative corrections in coherent elastic neutrino-nucleus scattering. *JHEP*, 02:097, 2021.
- [9] D. Cintas, P. An, C. Awe, P. S. Barbeau, E. Barbosa de Souza, S. Hedges, J. H. Jo, M. Martínez, R. H. Maruyama, L. Li, G. C. Rich, J. Runge, M. L. Sarsa, and W. G. Thompson. Quenching Factor consistency across several NaI(Tl) crystals. *Journal of Physics: Conference Series*, 2156(1):012065, dec 2021.
- [10] Belkis Cabrera-Palmer. Measurement of the low-energy germanium quenching factor with a small-mass detector. 10 2018.
- [11] C. Awe, P. S. Barbeau, J. I. Collar, S. Hedges, and L. Li. Liquid scintillator response to proton recoils in the 10–100 keV range. *Phys. Rev. C*, 98:045802, Oct 2018.
- [12] M. Abdullah et al. Coherent elastic neutrino-nucleus scattering: Terrestrial and astrophysical applications. 3 2022.
- [13] D. Akimov et al. The COHERENT Experimental Program. In *2022 Snowmass Summer Study*, 4 2022.
- [14] P. S. Barbeau, Yu. Efremenko, and K. Scholberg. COHERENT at the Spallation Neutron Source. 11 2021.
- [15] Ciaran A. J. O'Hare. New Definition of the Neutrino Floor for Direct Dark Matter Searches. *Phys. Rev. Lett.*, 127(25):251802, 2021.
- [16] Matteo Cadeddu, Carlo Giunti, Yufeng Li, and Yiyu Zhang. Average CsI neutron density distribution from COHERENT data. *PoS, NuFACT2018*:144, 2018.
- [17] Alessandro Mirizzi, Irene Tamborra, Hans-Thomas Janka, Ninetta Saviano, Kate Scholberg, Robert Bollig, Lorenz Hudepohl, and Sovan Chakraborty. Supernova Neutrinos: Production, Oscillations and Detection. *Riv. Nuovo Cim.*, 39(1-2):1–112, 2016.
- [18] Kate Scholberg. Supernova Neutrino Detection. *Ann. Rev. Nucl. Part. Sci.*, 62:81–103, 2012.
- [19] Georg G. Raffelt. Neutrinos and the stars. *Proc. Int. Sch. Phys. Fermi*, 182:61–143, 2012.
- [20] H. Th. Janka. Neutrino Emission from Supernovae. 2 2017.

- [21] D Z Freedman, D N Schramm, and D L Tubbs. The weak neutral current and its effects in stellar collapse. *Annual Review of Nuclear Science*, 27(1):167–207, 1977.
- [22] M. B. Tsang et al. Constraints on the symmetry energy and neutron skins from experiments and theory. *Phys. Rev. C*, 86:015803, 2012.
- [23] C. J. Horowitz and J. Piekarewicz. Neutron star structure and the neutron radius of Pb-208. *Phys. Rev. Lett.*, 86:5647, 2001.
- [24] Luca Baiotti. Gravitational waves from neutron star mergers and their relation to the nuclear equation of state. *Prog. Part. Nucl. Phys.*, 109:103714, 2019.
- [25] M. B. Tsang, W. G. Lynch, P. Danielewicz, and C. Y. Tsang. Symmetry energy constraints from GW170817 and laboratory experiments. *Phys. Lett. B*, 795:533–536, 2019.
- [26] COHERENT collaboration. Neutrino-Nucleus Inelastic Scattering at Low Energies with the COHERENT Experiment: A White Paper for the NSAC Long-Range Plan.
- [27] J. Asaadi et al. Physics Opportunities in the ORNL Spallation Neutron Source Second Target Station Era. In *2022 Snowmass Summer Study*, 9 2022.